The International Innovations Journal of Applied Science

Journal homepage: https://iijas.eventsgate.org/iijas

ISSN: 3009-1853 (Online)

Safety-Gated Multi-Band Sixth-Generation Vehicle-to-Everything Communication for Cooperative Autonomous Vehicles

Rawa Muayad Mahmood
Department of Electrical, College of Engineering, University of Tikrit, Iraq.

ARTICLE INFO

Article history:
Received 23 May 2026
Accepted 25 Aug. 2026
Available Online 2 Sep. 2026.

Keywords:
6G
Autonomous Vehicles
Vehicle-to-Everything
Multi-Connectivity
Sub-Terahertz

ABSTRACT

This research introduces a resource-conscious multi-band communication strategy for safety-sensitive collaborative messaging among autonomous cars utilizing sub-6 GHz, millimeter-wave, and sub-terahertz connections. A replicable Monte Carlo simulation assessed 120,000 urban-link instances encompassing communication ranges of 15–180 m, traffic densities of 10–120 vehicles/km, and precipitation rates of 0–35 mm/h. The model takes into account transmission, propagation, queuing, edge computing, shadowing, weather attenuation, obstruction, and recovery delays. The suggested policy was evaluated against fixed sub-6 GHz transmission, maximum-rate selection, RF-VLC-inspired link aggregation, and dynamic multi-connectivity. It duplicated 16.84% of packets, achieving a mean delay of 4.083 ms, a 95th percentile latency of 6.811 ms, and 99.298% delivery reliability within 10 ms. The dynamic multi-connectivity obtained 99.539% reliability but needed 26.31% duplication. The maximum-rate selection produced only 77.578% reliability due to blockage recovery. The results show that a sub-6 GHz anchor with selective high-band duplication provides a good trade-off between latency, reliability and resource consumption. These results are based on network-level simulations and do not prove road-safety certification or actual collision avoidance.

1. INTRODUCTION

Cooperative perception extends the visual range of an autonomous vehicle by sharing information about objects, trajectories and infrastructure sensing. Connectivity continues to be an improvement: localized sensing and a low-risk controller must preserve braking control. The challenge of the network is to provide updated information without relying on an unstable high-frequency connection.

The IMT-2030 framework delineates hyper-reliable low-latency communication, artificial intelligence in communication, and integrated sensing and communication as prospective application scenarios [1]. The report M.2541 investigates the viability beyond 100 GHz [2]. Neither document defines a specific 6G radio standard. In this paper, 6G-V2X is employed as a research framework that is aligned with those capabilities.

Sub-6 GHz ensures coverage and resilience against obstructions, but 28 GHz and 140 GHz deliver bandwidth but suffer from weather, range, and alignment vulnerabilities. The contribution is a safety-gated policy that maintains a strong anchor and replicates chosen messages across a beneficial high band. In contrast to a peak-rate selector, the aim clearly reveals dependability and the utilization of redundant resources.

The paper offers: (i) a clear multi-band cross-layer framework; (ii) a contextual gate including density, precipitation, distance, and anticipated obstruction costs; (iii) comparative analyses of common models against three established design principles; and (iv) empirical distributions, confidence intervals, and sensitivity maps. The reported result pertains to the promptness of communication, rather than the prevention of collisions.

* Corresponding author.
E-mail address: rawa.muayad@tu.edu.iq

2. RELATED WORK

According to Giordani et al. [3], Saad et al. [4], and Khan et al. [5], 6G may be seen as a blend of high frequency access, intelligence, sensing, and distributed computing. Yang et al. [6] investigate edge intelligence for autonomous driving while Mizmizi et al. [7] provide coordinated sensing for 6G mobility.
Singh et al combine radio frequency and visible light communications for dependable low latency V2X [8]. In the domain of mobility, Mishra et al. investigate packet duplication with dual connection [9]. Mahmood and Alves dynamically enable multi-connectivity for reducing resources [10]. In the current work these design rules are translated to a common three-band RF-model. It does not aim at an exact numerical reproduction, since their channels, carriers and activation rules are different.

3. MATERIALS AND METHODS

3.1 Architecture and Frequency Roles

Table 1. show the Functional frequency assignment based on the band , the bandwidth and the role.

Table 1. Functional frequency assignment.

Band	Bandwidth	Role
3.5 GHz	100 MHz	Safety anchor
28 GHz	800 MHz	Conditional capacity
140 GHz	2 GHz	Short-range opportunity

Vehicles exchange cooperative-perception packets with a roadside edge node. The edge can fuse sensing or maps, but emergency control remains local. A packet sent on band b experiences:

T_b=L/R_b+d/c+T_q +T_edge+I_bT_rec,b (1)

where L/Rb is transmission time, d/c propagation, Tq queueing, Tedge edge processing, and the final term blockage recovery. Rate is capped to avoid unrealistic Shannon throughput:

R_b=B_b min[log_2(1+10^(SNR _b/10)), eta_max,b] (2)

Free-space loss, log-normal shadowing, receiver noise, and frequency-dependent rainfall contribute to SNR. Blockage probability is:

p_blk,b=clip(a_b+bet a_b rho+gamma_b r,0,0.65) (3)

with density rho and rainfall r. The affine abstraction is auditable but cannot replace a geometry-based or measured vehicular channel.

3.2 Proposed Safety-Gated Multi-Connectivity

The anchor risk score is its predicted base latency plus expected recovery cost. A 28 GHz copy is eligible below 90 vehicles/km, 25 mm/h, and 160 m. A 140 GHz copy is eligible below 45 vehicles/km, 8 mm/h, and 85 m. Duplication is activated only when anchor risk exceeds 4.4 ms. The high band with lower expected base-plus-blockage cost is used, and the earliest copy is retained:

T_prop=min(T_sub6,T_h) if gate=1; otherwise T_sub6* (4)

This differs from always-on aggregation by pricing duplicate-resource use, and from rate maximization by preserving the anchor. Thresholds were fixed before the final evaluation run and are exposed in the source code.

3.3 Comparison Policies

Table 2. Policies. Literature baselines are principle-level emulations.

Policy	Common-model implementation
Fixed sub-6	Anchor only
Max-rate	Smallest predicted unblocked latency
LA-inspired [8]	Parallel 28/140 GHz copies
Dynamic MC [10]	Duplicate when anchor risk >5 ms
Proposed	Context gate plus anchor duplication

3.4 Simulation Parameters and Statistical Analysis

NumPy with seed 2030 was used to generate 120,000 independent link realizations. Distance was constant between 15-180 m, density between 10-120 vehicles/km, and rainfall between 0-35 mm/h. The payload followed a lognormal distribution with median 0.8 Mbit and log deviation 0.45. Edge time was truncated normal with mean 1.2 ms. Queueing was exponential with mean dependant on density.

Table 3. Model assumptions; they are not measurements.

Parameter	3.5 GHz	28 GHz	140 GHz
Tx power	23 dBm	26 dBm	20 dBm
Gain	6 dB	24 dB	34 dB
Noise figure	7 dB	8 dB	10 dB
Shadow sigma	3 dB	5.5 dB	7 dB
Efficiency cap	5.5	7	8 b/s/Hz
Base blockage	0.003	0.035	0.070
Recovery	8+Exp(4)	18+Exp(4)	30+Exp(4) ms

The main objective was the percentage provided within a 10 ms communication budget. Mean and 95th-percentile latencies and duplicate-packet percentages were secondary endpoints. The sample was split into 30 groups of 4,000. The given 95% CI for each statistic is the batch mean ±1.96 standard errors. The empirical CDF employs all the realizations. Sensitivity cells marginalize over density and provide the observed miss percentage in each distance-rain bin.

As all the policies are tested on the same produced channel states, the comparisons are at the scenario level. A hypothesis test does not transform model assumptions into physical evidence. Monte Carlo uncertainty is only quantified by confidence intervals.

4. RESULTS

Table 4. Mean ± 95% CI half-width across 30 batches.

Policy	**Mean ms**	**P95 ms**	**10-ms rel.**	**Dup.**
Fixed sub-6	4.368±.010	7.197±.037	99.123±.055%	0%
Max-rate	9.808±.076	38.030±.093	77.578±.228%	0%
LA-inspired	3.781±.024	7.992±.831	95.662±.104%	100%
Dynamic MC	3.926±.007	5.880±.037	99.539±.033%	26.31%
Proposed	4.083±.010	6.811±.036	99.298±.047%	16.84%

The selection of maximum rates is suboptimal at the tail as it fails to account for blockage recovery. The elevated-band replication influenced by LA reduces the average latency, yet neglects the anchor and does not meet 4.338% of the 10 ms deadlines. Optimal dependability with dynamic MC, yet it replicates 26.31% of packets. The suggested policy diminishes redundancy by 36.0% relative to dynamic MC, with a reliability decrease of 0.241 percentage points.

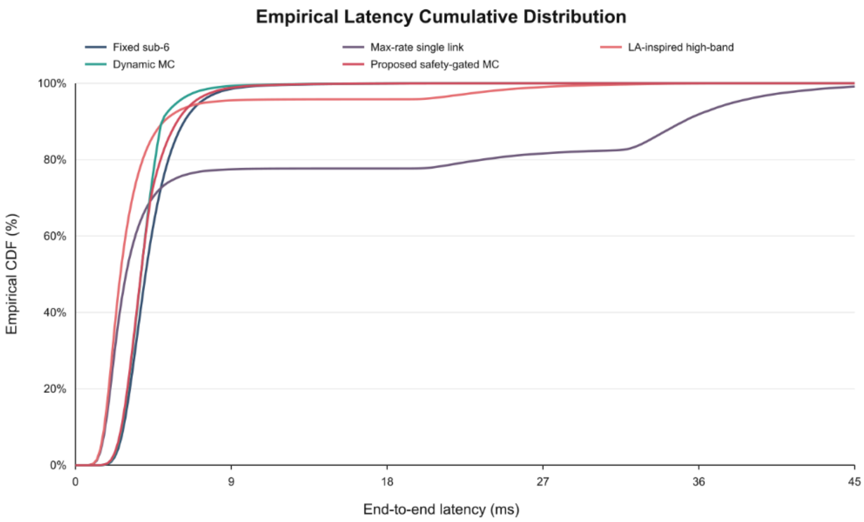

Figure 1. Empirical latency CDF. The inset-free distribution exposes tail behavior rather than a bar summary.

DOI: https://doi.org/10.61856/f3dbqm84

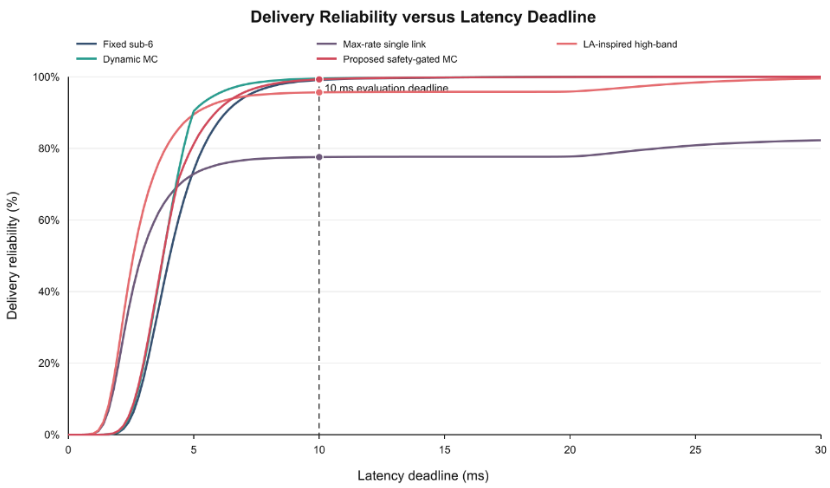

Figure 2. Delivery reliability versus latency deadline for the evaluated communication policies. The dashed vertical line and markers indicate the reliability achieved by each policy at the 10 ms evaluation deadline.

Figures 1 and 2 show the shortcoming of a single mean. The max-rate curve has a long recovery tail whereas multi-connectivity policies re-distribute probability mass towards low delay. Dynamic MC is the first, then the proposed method and fixed sub-6 at the 10 ms vertical interpretation point. The proposed curve approximates dynamic MC but needs less duplicate transmissions.

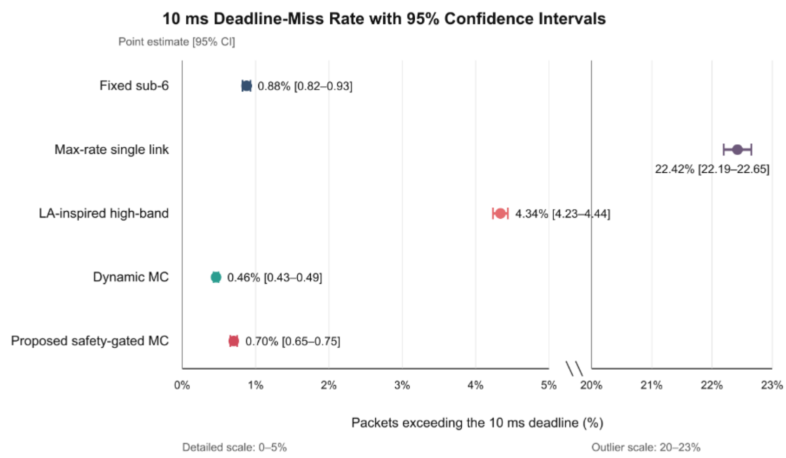

Figure 3. Ten-millisecond deadline-miss estimates with batch-based 95% confidence intervals.

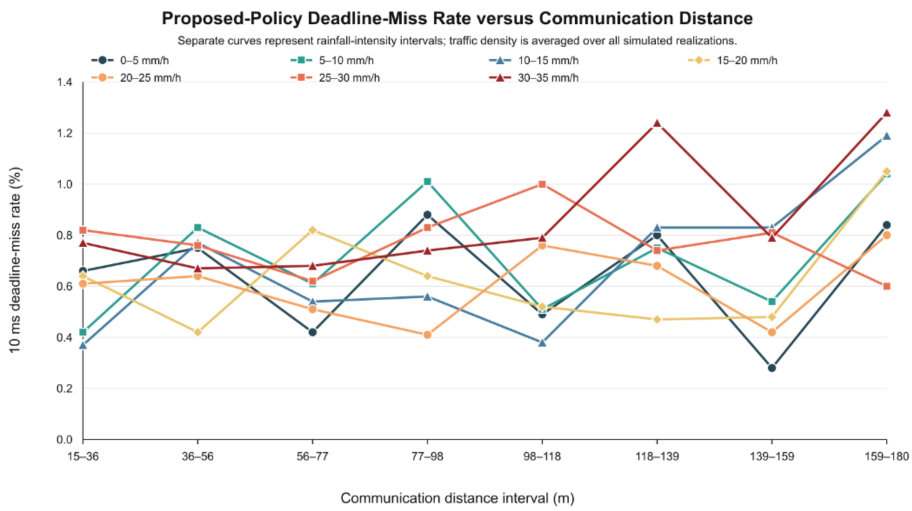

Figure 4. Proposed-policy deadline-miss percentage by distance and rainfall; density is marginalized.

Figure 3's narrow intervals suggest that the Monte Carlo sampling error is negligible in comparison to policy differences. They do not consider structural uncertainty in path-loss, blockage or queue models. Figure 4 illustrates the operating regions in which the anchor is becoming more dominant due to the fact that high-frequency eligibility is bound by distance and precipitation.

5. DISCUSSION

5.1 Engineering Interpretation

\The results refute the assumption that selecting the nominally fastest carrier is adequate for safety traffic. Recovery penalties render high-band-only policies vulnerable. Consequently, a robust anchor is not legacy overhead; it is a diversity component. The operator's duplicate-resource budget determines the choice between dynamic MC and the proposed gate. If 0.24 percentage points of additional 10 ms reliability justify approximately 56% more duplication relative to the proposed policy, dynamic MC is preferable. Under tighter spectral or energy budgets, the proposed method is the more balanced solution.

The 140 GHz layer is utilized exclusively at short range and benign weather. It should support feature bursts, sensing, or redundant delivery, rather than serve as the sole emergency bearer. This conclusion is consistent with feasibility studies above 100 GHz [2] and packet-duplication literature [9-11].

5.2 Relation to Published Baselines

The LA-inspired policy employs the parallel-link reliability principle of Singh et al. [8], but substitutes VLC by two high RF-bands. The MC is dynamic and follows the selective-activation principle of Mahmood and Alves [10]. Mishra et al. [9] and Rao and Vrzic [11] further support always-on and optimized packet duplication. These are controlled baselines at the principle level, not claims that the same numerical values were reported in the original papers.

5.3 Limitations and Validity

This is a Monte Carlo simulation at the network level. This is not SUMO, CARLA, ns-3, Simu5G, a channel-sounder experiment, or a road trial. Independent snapshots ignore the temporal correlation of blockages, beam-training dynamics, handovers, interference coordination and detailed MAC scheduling. Assumptions are the affine blockage law and recovery times. Thus, the results are in favor of comparative algorithm reasoning under a declared model, but do not prove that collisions are avoided.

Future validation should: (1) import time-correlated trajectories, (2) use standardized IMT-2030 evaluation channels once finalized, (3) calibrate rain and blockage using measured traces, and (4) connect age-of-information to a vehicle controller. A hardware-in-the-loop experiment would be required before any functional-safety claim.

5.4 Reproducibility

Policy gates, batch confidence intervals, CSV output, figure generation, parameters, seed, and equations are all included in the accompanying script. No proprietary data used. This allows reviewers to change thresholds or to revise channel assumptions without the reliance of hidden findings.

6. CONCLUSION

For cooperative autonomous vehicle communication , a safety-gated multi-band policy was assessed. The technique maintains sub-6 GHz and enables a 28 or 140 GHz replica only when context and anchor risk warrant it. It obtained 99.298% delivery within 10 ms with 16.84% duplication rate. Dynamic MC attained 99.539%, it incurred a 26.31% duplication rate, suggesting a clear trade-off between dependability and resource efficiency. Moreover, the high-frequency spectrum is better understood as a context-dependent layer of variety and capacity, rather than as a singular safety carrier.

Conflict of Interest: The author declares that no conflict of interests.

Funding: No external funding was used for this simulation study.

Data and Code Availability: The reproducible Python source and generated numerical CSV are supplied with the manuscript.

REFERENCES

[1] ITU-R (2023), Framework and overall objectives of the future development of IMT for 2030 and beyond. Recommendation M.2160-0.

[2] ITU-R (2024), Technical feasibility of IMT in bands above 100 GHz. Report M.2541-0.

[3] Giordani M, Polese M, Mezzavilla M, Rangan S, Zorzi M (2020), Toward 6G networks: Use cases and technologies. IEEE Commun Mag 58(3), 55-61. DOI: 10.1109/MCOM.001.1900411.

[4] Saad W, Bennis M, Chen M (2020), A vision of 6G wireless systems. IEEE Netw 34(3), 134-142. DOI: 10.1109/MNET.001.1900287.

[5] Khan LU, Yaqoob I, Imran M, Han Z, Hong CS (2020), 6G wireless systems: A vision, architectural elements, and future directions. IEEE Access 8, 147029-147044. DOI: 10.1109/ACCESS.2020.3015289.

[6] Yang B et al. (2021), Edge intelligence for autonomous driving in 6G wireless system. IEEE Wireless Commun 28(2), 40-47. DOI: 10.1109/MWC.001.2000292.

[7] Mizmizi M et al. (2021), 6G V2X technologies and orchestrated sensing for autonomous driving. arXiv:2106.16146.

[8] Singh G et al. (2024), Toward 6G-V2X: Aggregated RF-VLC for ultra-reliable and low-latency autonomous driving. IEEE Commun Standards Mag 8(4), 80-87. DOI: 10.1109/MCOMSTD.0001.2300005.

[9] Mishra P, Kar S, Wang KC (2022), Performance evaluation of 5G multi-connectivity with packet duplication for reliable low latency communication in mobility scenarios. IEEE VTC-Spring. DOI: 10.1109/VTC2022-Spring54318.2022.9860634.

[10] Mahmood NH, Alves H (2019), Dynamic multi-connectivity activation for ultra-reliable and low-latency communication. ISWCS, 112-116. DOI: 10.1109/ISWCS.2019.8877325.

[11] Rao J, Vrzic S (2018), Packet duplication for URLLC in 5G: Architectural enhancements and performance analysis. IEEE Netw 32(2), 32-40. DOI: 10.1109/MNET.2018.1700227.

[12] Xiong K, Leng S, Chen X, Huang C, Yuen C, Guan YL (2020), Communication and computing resource optimization for connected autonomous driving. IEEE Trans Veh Technol 69(11), 12652-12663. DOI: 10.1109/TVT.2020.3029109.

[13] Tataria H et al. (2021), 6G wireless systems: Vision, requirements, challenges, insights, and opportunities. Proc IEEE 109(7), 1166-1199. DOI: 10.1109/JPROC.2021.3061701.